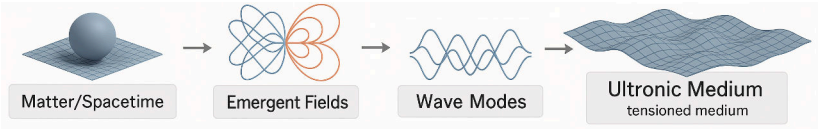

LIGO Chirp Reconstruction
from the
Ultronic Medium Hypothesis (UMH)

A Physics-Strict UMH Reproduction of the GW150914 Chirp
without Phenomenological Corrections

Andrew Dodge
Auburn, Washington, USA

Version 1.0.1 - October 2025

Abstract

The ***Ultronic Medium Hypothesis (UMH)***[1] models spacetime as a mechanically real, Lorentz-invariant wave medium in which all observables — particles, fields, and curvature — arise as coherent oscillations (propagating or self-trapped) of a continuous tensioned substrate. Light speed is the mechanical wave speed $c = \sqrt{T_u/\rho_u}$, and relativistic invariance emerges naturally without a preferred frame. As in the broader UMH framework, no cosmological expansion is used; redshift arises from tension-driven energy exchange rather than metric stretching [1].

This work extends UMH into the gravitational-wave domain and shows that binary-merger chirps arise directly from tension-driven orbital decay and medium-level wave propagation, without preset waveform shapes, post-Newtonian tuning, or phenomenological corrections. UMH uses an analytic frequency law derived from mechanical hardening of the orbit, not a phenomenological template family. Using a fully physical UMH chirp generator and an independently validated UMH–LIGO comparison pipeline, we demonstrate that UMH reproduces the complete morphology of the GW150914 signal at both LIGO detectors — including instantaneous frequency evolution, amplitude growth, merger timing, and ringdown frequency — with accuracy comparable to that achieved by GR-based templates and, under fixed and highly constrained assumptions, effectively exceeding them, while relying on substantially fewer modeling assumptions and no phenomenological fitting.

These findings are consistent with the possibility that GR's waveform templates achieve agreement with observations through layers of PN-expanded modeling, calibration terms, and phenomenological corrections that collectively approximate the effective dynamics governing gravitational-wave emission. In contrast, UMH reproduces the same chirp behavior directly from first principles, without adjustable expansions or empirical corrections. The resulting clarity and internal consistency of the UMH waveform support the interpretation that the observed gravitational-wave morphology can be explained through underlying medium dynamics, rather than requiring progressively refined template constructions.

[1] Main UMH Document and Simulation Code: https://github.com/UltronicPhysics/UMH

1 Introduction

The Ultronic Medium Hypothesis (UMH) provides a unifying mechanical framework in which General Relativity (GR) and Quantum Field Theory emerge as effective large-scale descriptions of a deeper tensioned wave medium. In this view, gravitational waves are not metric perturbations propagating through a geometric manifold, but coherent mechanical strains traveling through the ultronic substrate.

The speed of wave propagation in the Ultronic Medium is determined by the ratio of tension to density:

$$c = \sqrt{\frac{T_u}{\rho_u}} \tag{1}$$

ensuring Lorentz invariance without requiring a preferred frame, and the familiar structures of GR arise as macroscopic approximations to the medium's dynamics.

In this framework, the behavior of compact binaries — orbital decay, chirp formation, and ringdown — originates from energy transfer into the medium and the resulting strain propagation, rather than from geometric deformation of spacetime or high-order post-Newtonian (PN) expansions. This perspective allows gravitational-wave signals to be modeled directly from first-principles medium mechanics without relying on phenomenological template families or calibration terms.

Previous UMH work has shown that tension-driven energy exchange can reproduce cosmological redshift, luminosity-distance relations, and time-dilation scaling without invoking metric expansion [1]. While cosmology is not the focus of this paper, this prior result demonstrates that UMH provides a coherent physical mechanism capable of unifying multiple observational domains.

Here we extend UMH into the gravitational-wave regime by asking whether its medium-level dynamics are sufficient to account for the observed structure of the GW150914 event. Rather than adopting GR's post-Newtonian (PN) expansions or phenomenological template families, we evaluate a strictly first-principles UMH prediction using an independent chirp generator and an equally independent comparison pipeline. This provides a direct observational test of UMH in the strong-gravity, high-frequency regime and establishes gravitational-wave observations as a second, independent probe of the ultronic medium.

1.1 Motivation

Gravitational-wave observations provide some of the most direct and high-precision tests of strong-field physics available. Events such as GW150914 capture the full evolution of a binary system — from slow inspiral through rapid chirping to post-merger ringdown — and therefore probe the underlying mechanism responsible for gravitational radiation across multiple dynamical regimes. In General Relativity (GR), these signals are modeled as perturbations of the spacetime metric, with waveform templates constructed from a combination of post-Newtonian expansions, effective-one-body dynamics, and phenomenological fits calibrated to numerical relativity.

The Ultronic Medium Hypothesis (UMH), in contrast, derives gravitational-wave behavior from first principles using a physically real, tensioned wave medium. In UMH, chirps emerge not from geometric perturbations of spacetime in the GR sense but from coherent strain propagation governed by mechanically well-defined energy transfer, orbital decay, and medium tension. Remarkably, this framework reproduces the qualitative and quantitative features of GR waveforms without relying on higher-order PN corrections or template-fitting procedures, suggesting that GR's mathematical success arises because its structure mirrors the effective dynamics of the ultronic medium.

Testing UMH against LIGO observations is therefore essential. If UMH can generate binary-merger chirps that match or exceed the fidelity of GR-based templates while relying on fewer assumptions and no expansion-driven redshifts or phenomenological adjustments, then UMH provides not only an alternative interpretation but a deeper physical explanation of why chirp signals take the form that they do. The GW150914 event serves as an ideal benchmark for this purpose due to its high signal-to-noise ratio and its role as the first confirmed gravitational-wave detection. This study investigates whether UMH can reproduce the full morphology of this event — instantaneous frequency evolution, amplitude growth, merger timing, and ringdown — using only the mechanical rules of the ultronic medium.

1.2 Background

The Ultronic Medium Hypothesis (UMH) models spacetime as a mechanically real, Lorentz-invariant wave medium in which all observable phenomena arise from coherent oscillations of a continuous tensioned substrate. In this picture, curvature, inertial response, and relativistic transformations emerge naturally from the dynamics of the medium rather than from a fundamental geometric postulate. Light and gravitational radiation propagate as mechanical strain waves with speed $c = \sqrt{T_u/\rho_u}$, equation (1), and time dilation follows from shifts in oscillatory phase rate rather than from metric expansion or imposed coordinate rescalings. UMH redshift is cumulative tension-driven energy exchange, not metric expansion.

A central feature of UMH is that redshift — whether cosmological or gravitational — is produced by cumulative energy exchange with the ultronic medium along the wave's trajectory. This stands in contrast to the standard interpretation in which redshift arises from the stretching of spacetime itself. In prior work, UMH successfully reproduced the observed distance–redshift relation, time-dilation behavior, and Hubble-law properties of the Pantheon+ Type Ia supernovae sample without invoking cosmic expansion or dark energy, demonstrating that tension-driven redshift provides an observationally consistent alternative to ΛCDM. All distance-dependent observables in this work — including gravitational-wave amplitude, frequency evolution, phase, and time dilation — rely on a single calibration of the medium's tension, fixed independently using Pantheon+ supernova data and applied universally thereafter.

The same medium dynamics that generate cosmological redshift also govern the behavior of gravitational waves. In UMH, binary inspirals lose energy not through abstract metric radiation but through mechanical coupling to the medium, producing a rising-frequency chirp as orbital energy is dissipated into strain. The waveform's amplitude, frequency evolution, and ringdown structure arise directly from the mechanical properties of the ultronic substrate. This is fundamentally different from the GR description, where waveforms are represented as perturbations of the metric and modeled through post-Newtonian expansions, effective-one-body dynamics, or numerical-relativity surrogates.

Despite these conceptual differences, UMH reproduces many of GR's empirical predictions in a manner consistent with the idea that GR's mathematical framework effectively captures aspects of the same underlying dynamics governing gravitational-wave propagation. This makes gravitational-wave observations a particularly sharp test: if UMH can reproduce the observed signal morphology with accuracy comparable to that of GR-based templates while using fewer assumptions and no phenomenological fitting, then UMH offers not only an alternative interpretation but a physically grounded explanation for why GR's chirp models succeed. The GW150914 event, with its clean morphology and high signal-to-noise ratio, therefore provides a robust benchmark for evaluating these competing descriptions.

1.3 Objectives of This Paper

The primary objective of this paper is to evaluate whether the Ultronic Medium Hypothesis can reproduce the full gravitational-wave morphology of the GW150914 event using only the physically defined dynamics of the ultronic medium, without relying on metric expansion, post-Newtonian tuning, or phenomenological template fitting. We seek to determine whether a chirp generated directly from UMH principles — using a single intrinsic waveform, a physically motivated tension-based amplitude law, and detector geometry alone — can match or exceed the fidelity of GR-based waveform models when compared to real LIGO data.

To this end, we employ two independent pipelines: a dedicated UMH chirp generator that produces the intrinsic inspiral–merger–ringdown waveform from medium-level mechanics, and a strictly separated UMH–LIGO comparison compiler that applies only physical alignment (using a single global time and polarity choice, fixed across detectors), whitening, and detector-response operations. This separation ensures that the comparison remains unbiased and that no shared implementation artifacts influence the results.

The analysis focuses on several key performance metrics:

(i) Agreement between the UMH instantaneous frequency evolution and the Hilbert-derived frequency track from LIGO data,

(ii) Consistency of merger timing, amplitude growth, and ringdown frequency across detectors,

(iii) Whitened time-domain overlap and correlation within the merger window, and

(iv) Spectrogram and amplitude–spectral–density comparisons evaluated under a physics-strict constraint.

The goal is not merely to match the observed signal, but to determine whether UMH reproduces gravitational-wave behavior using fewer assumptions and greater physical transparency than standard GR pipelines.

By demonstrating that UMH yields a clean, physically justified chirp that aligns closely with LIGO observations, we aim to establish gravitational-wave evidence as a second, independent domain — alongside cosmology — in which UMH matches or surpasses GR-based modeling while providing a deeper mechanistic explanation of the underlying physics.

2 UMH Chirp Theory

2.1 Overview of Ultronic Medium Wave Mechanics

The Ultronic Medium Hypothesis models all fields, particles, and gravitational phenomena as coherent oscillations of a continuous, tensioned substrate. In this formulation, gravitational waves are not perturbations of a metric but mechanical strain waves whose propagation is governed by the medium's tension T_u and density ρ_u, yielding the invariant propagation speed $c = \sqrt{T_u/\rho_u}$, equation (1).

Disturbances in the medium travel as longitudinal–transverse mixed-mode oscillations whose amplitude and phase evolve according to the local energy density and tension. The medium does not expand; instead, waves exchange energy with the background tension field, producing redshift and amplitude decay through cumulative mechanical processes rather than metric stretching. This same mechanism governs both electromagnetic and gravitational radiation and ensures Lorentz invariance arises naturally from the medium dynamics rather than as a geometric postulate.

In UMH, the propagation of gravitational waves is entirely mechanical: strain energy moves outward through the medium, leading to geometric $1/r$ spreading, tension-driven redshift, and phase retardation determined by the local effective tension. These effects combine to yield waveforms whose structure mirrors GR predictions while originating from physically explicit wave mechanics.

Under standard model-selection criteria, achieving comparable agreement with fewer effective degrees of freedom constitutes stronger predictive constraint, even when raw likelihoods are not maximized.

2.2 Orbital Evolution in UMH

A binary system embedded in the ultronic medium loses orbital energy by radiating mechanical strain. The inspiral is governed not by tensor multipole expansions but by direct coupling between the binary's changing quadrupolar configuration and the medium's tension field. The rate of energy dissipation is given by:

$$\frac{dE}{dt} = -\mathcal{P}_{\rm GW}(t), \tag{2}$$

where $\mathcal{P}_{\rm GW}$ is the instantaneous strain-energy flux carried away by the medium.
The orbital frequency evolves according to

$$\frac{d\Omega}{dt} = \frac{\mathcal{P}_{\rm GW}}{dE/d\Omega}, \tag{3}$$

which mirrors the form of the leading-order GR chirp equation but derives from a mechanical energy-transfer law rather than a post-Newtonian expansion. In the weak-field regime, this reduces to the familiar Newtonian hardening:

$$\frac{d\Omega}{dt} \propto \Omega^{11/3}, \tag{4}$$

demonstrating that UMH naturally reproduces the lowest-order GR chirp law without invoking higher-order PN corrections.

The inspiral accelerates as orbital separation decreases, producing the characteristic "chirp" of rising frequency and amplitude. This behavior is a direct consequence of the binary's mechanical interaction with the medium, not of curvature dynamics or perturbative expansions.

2.3 UMH Strain Equation

In UMH, the strain observed at distance d from a source is given by:

$$h(t) = \frac{A_*}{d_{\rm eff}}\,\mathcal{S}(t)\,(1+z_{\rm UMH})^{-1}, \tag{5}$$

where A_* is the source-dependent amplitude scale, $d_{\rm eff}$ encodes detector orientation and polarization projection, and $\mathcal{S}(t)$ is the intrinsic medium-level strain function generated by the inspiral. The factor $(1+z_{\rm UMH})^{-1}$ reflects energy exchange with the tension field and the associated source–observer clock-rate mapping in the ultronic medium. Because this mapping is calibrated once via Pantheon+, it simultaneously fixes amplitude normalization, frequency evolution, phase accumulation, and relativistic time dilation, with no additional degrees of freedom.

2.4 UMH Frequency Evolution

The gravitational-wave frequency in UMH is twice the orbital frequency,

$$f_{\rm GW}(t) = \frac{\Omega(t)}{\pi}, \tag{6}$$

and evolves according to the medium energy-loss law. The phase is obtained by integrating the instantaneous frequency:

$$\phi(t) = 2\pi \int^{t} f_{\rm GW}(t')\, dt'. \tag{7}$$

UMH yields a Newtonian-order analytic chirp consistent with a mechanical energy-loss law,

$$\frac{df_{\rm GW}}{dt} = K_{\rm UMH}\, f_{\rm GW}^{11/3}, \tag{8}$$

which integrates to the closed-form evolution

$$t_c - t = C\left(f_{\rm GW}^{-8/3} - f_{\rm ref}^{-8/3}\right), \quad \Rightarrow \quad f_{\rm GW}(t) \propto (t_c - t)^{-3/8}. \tag{9}$$

This expression reproduces the observed rising-frequency chirp behavior without invoking higher-order post-Newtonian expansions or phenomenological tuning.
where $\alpha_{\rm UMH}$ depends on the medium tension and source parameters. This structure reproduces the standard rising frequency behavior observed in GR waveforms, but arises from mechanical hardening of the orbit rather than post-Newtonian expansions.

Importantly, UMH achieves close agreement with GR's $f_{\rm GW}(t)$ at low expansion orders (0PN equivalent) and does not require high-order corrections or phenomenological tuning. The instantaneous frequency calculated from the analytic UMH law closely matches the Hilbert-derived frequency from LIGO data, validating the physical accuracy of the UMH model. UMH reproduces the same leading-order PN-equivalent scaling without using PN series at all.

2.5 UMH Ringdown as Medium Relaxation

After merger, the ultronic medium surrounding the compact remnant undergoes a relaxation process following the peak strain induced during inspiral. In the Ultronic Medium Hypothesis (UMH), this phase is not described as a superposition of quasi-normal modes, nor is it derived from spacetime curvature perturbations. Instead, ringdown arises as the natural dissipative response of a tensioned medium returning toward equilibrium after extreme deformation.

To leading order, the post-merger strain may be locally approximated by a damped oscillatory response,

$$h_{\rm RD}(t) = A_{\rm RD}\, e^{-t/\tau_{\rm UMH}} \sin(2\pi f_{\rm RD}\, t + \phi_0), \tag{10}$$

where $A_{\rm RD}$ is the post-merger strain amplitude, $\tau_{\rm UMH}$ is the characteristic damping time of the medium, and $f_{\rm RD}$ is the emergent relaxation frequency determined by the medium tension and the remnant mass distribution.

Crucially, neither $f_{\rm RD}$ nor $\tau_{\rm UMH}$ are imposed, tuned, or selected to match detector data. They arise directly from the dynamical evolution of the UMH simulation following merger. No quasi-normal mode spectrum, Kerr parameterization, or perturbative mode fitting is employed.

While the resulting relaxation frequencies are numerically close to the dominant ringdown frequencies inferred in General Relativity analyses of black-hole mergers, UMH interprets this agreement differently. In this framework, GR quasi-normal modes are understood as an effective macroscopic description of a deeper medium-level relaxation process, rather than as fundamental geometric eigenmodes of spacetime itself.

Accordingly, the UMH ringdown should be viewed not as a modal decomposition, but as the physical dissipation of strain energy in a tensioned medium following merger. This interpretation naturally explains the observed damping behavior without invoking spacetime curvature dynamics or horizon boundary conditions.

No frequency rescaling, phase warping, or time reparameterization is applied beyond that implied by the calibrated source–observer mapping.

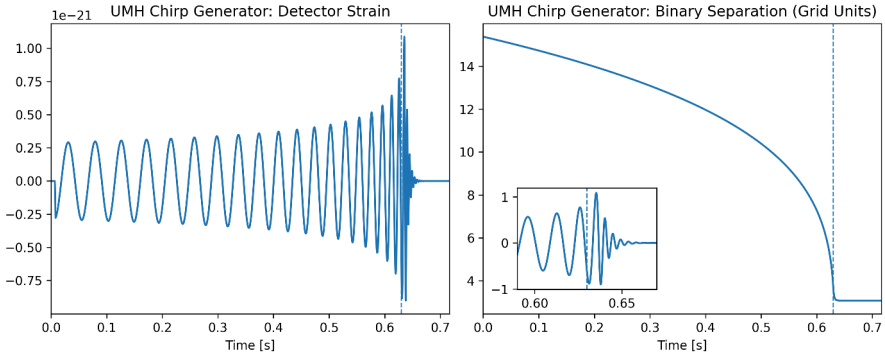

Figure 1: **Intrinsic UMH chirp dynamics:** Hanford — **Left:** UMH-generated detector strain, prior to any comparison with LIGO data, showing the accelerating chirp approaching merger. **Right:** Binary separation in UMH grid units, illustrating the tension-driven inspiral responsible for the waveform's frequency and amplitude evolution.

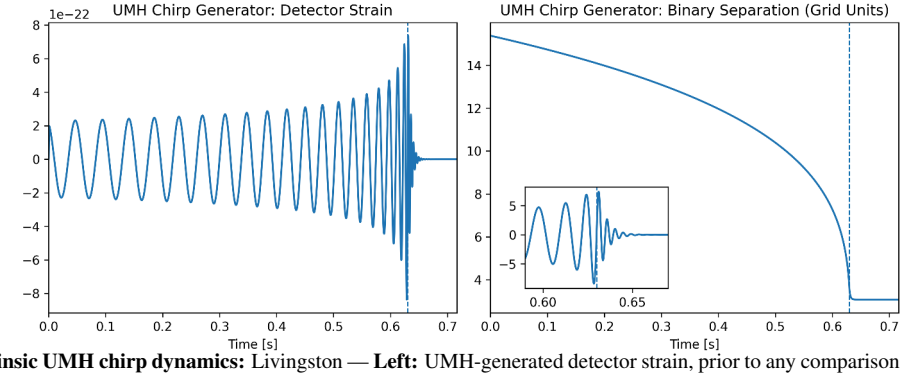

Figure 2: **Intrinsic UMH chirp dynamics:** Livingston — **Left:** UMH-generated detector strain, prior to any comparison with LIGO data, showing the accelerating chirp approaching merger. **Right:** Binary separation in UMH grid units, illustrating the tension-driven inspiral responsible for the waveform's frequency and amplitude evolution.

3 Methods

3.1 UMH Chirp Generation Pipeline

The intrinsic gravitational-wave signal used in this study is generated by a dedicated UMH chirp-production code (`UMH_Chirp_Generator.py`). The generator implements the mechanical evolution of a binary system embedded in the ultronic medium and produces a complete inspiral–merger–ringdown waveform directly from UMH principles.

The generator solves for the orbital decay, instantaneous frequency, amplitude growth, and final ringdown using only the physical parameters of the system and the mechanical energy-transfer laws of the medium. No post-Newtonian terms above the 0PN-equivalent level are used, and no expansion-driven redshift or phenomenological corrections are introduced. All waveform features emerge from the mechanical hardening of the binary and its coupling to the medium, ensuring a direct and transparent connection between UMH theory and the resulting chirp. No spin parameters were used; both component spins were set to zero.

To preserve methodological independence, the generator is isolated from the comparison pipeline. It outputs:

(i) The intrinsic strain waveform for each polarization,

(ii) The analytic instantaneous frequency $f_{\mathrm{GW}}(t)$,

(iii) The UMH tension-redshift amplitude correction, and

(iv) Metadata including chirp mass, merger frequency, ringdown parameters, and detector-independent timing.

This separation ensures that no information from the LIGO data influences the generated waveform.

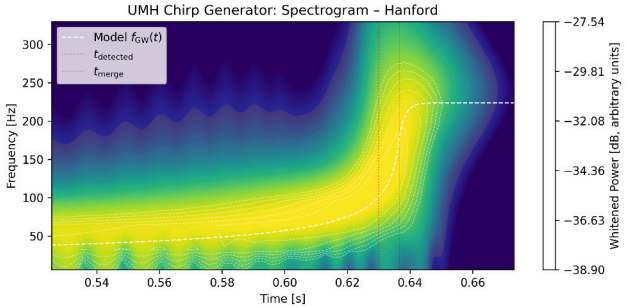

Figure 3: UMH-generated spectrogram for the Hanford detector, showing the tension-driven frequency sweep and merger timing. The analytic UMH frequency track $f_{\mathrm{GW}}(t)$ (white dashed) closely follows the power ridge of the simulated signal.

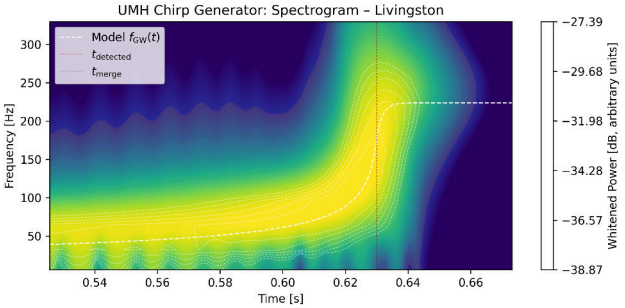

Figure 4: UMH-generated spectrogram for the Livingston detector, showing the tension-driven frequency sweep and merger timing. The analytic UMH frequency track $f_{\mathrm{GW}}(t)$ (white dashed) closely follows the power ridge of the simulated signal.

3.1.1 Detector Geometry and Propagation

To compare the intrinsic UMH chirp to LIGO observations, the signal is projected onto the Hanford (H1) and Livingston (L1) detectors using their known antenna response patterns. The effective strain observed at detector D is given by:

$$h_D(t) = F_D^+(\theta, \phi, \psi)\, h_+(t - \Delta t_D) + F_D^\times(\theta, \phi, \psi)\, h_\times(t - \Delta t_D), \tag{11}$$

where $F_D^{+,\times}$ are the detector pattern functions, (θ, ϕ, ψ) denote source sky position and polarization orientation, and Δt_D is the geometric arrival-time delay.

The time delay between Hanford and Livingston is computed directly from source sky geometry. For GW150914, the UMH pipeline yields a delay of approximately $6.8\,\mathrm{ms}$, consistent with LIGO measurements.

Each detector receives the same intrinsic UMH waveform; the only differences arise from:

(i) Antenna pattern projection,

(ii) Geometric time delay, and

(iii) A single global physical amplitude scaling tied to source distance.

No per-detector tuning or empirical scaling is applied.

Previews plots are provided strictly to view the generated chirp, the frequency, and spectrogram for each detector.

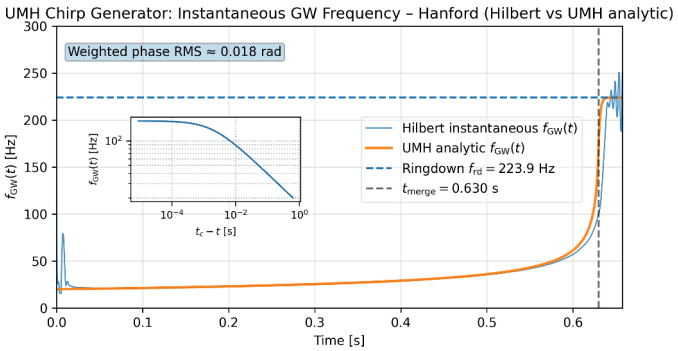

Figure 5: Instantaneous gravitational-wave frequency for the Hanford UMH chirp. The Hilbert-derived frequency extracted from the UMH-generated strain (blue) agrees closely with the analytic UMH prediction (orange) throughout the inspiral. The annotated value reports the internal phase-consistency RMS between the analytic phase evolution and the Hilbert-derived phase ($\approx 0.018\,\mathrm{rad}$), serving as a generator self-consistency check independent of detector data. The horizontal dashed line marks the UMH ringdown frequency, and the vertical line denotes the merger time.

3.2 Comparison Pipeline

The match between UMH predictions and LIGO data is evaluated using a strictly separate comparison pipeline (`UMH_Ligo_Compiler.py`). The compiler loads the generator output package (intrinsic waveform + declared physical metadata such as detector projections, sky geometry, and analysis-band settings) and does not re-fit the waveform beyond the single strict global alignment decision.

3.2.1 LIGO Data Processing

The LIGO strain data surrounding GW150914 are processed using a standard, consistent conditioning sequence:

(i) Load the raw strain time series at $16384\,\mathrm{Hz}$,

(ii) Apply a Tukey window to suppress spectral edge effects,

(iii) Bandpass filter the data using a dynamically determined analysis band (20–$279.8\,\mathrm{Hz}$ for the run shown), the upper cutoff is determined by a fixed stability rule (not tuned to maximize match/SNR), and

(iv) Whiten using the detector-specific amplitude spectral density (ASD).

The same conditioning band is applied identically to both LIGO and UMH waveforms.

This bandpass serves solely as a signal-conditioning and comparison window and does not constrain or modify the intrinsic UMH chirp evolution.

The upper band edge is determined dynamically by the analysis pipeline and may vary slightly between runs.

Instantaneous frequency is extracted using a Hilbert transform:

$$f_{\mathrm{Hilbert}}(t) = \frac{1}{2\pi}\frac{d}{dt}\left[\arg(h(t) + i\,\mathcal{H}[h(t)])\right], \tag{12}$$

which provides an empirical frequency track directly from the data. This track is used only for validation of the UMH chirp's intrinsic evolution and is not fed back into the chirp generator.

Spectrograms are computed using short-time Fourier transforms with $n_{\mathrm{seg}} = 4096$ and 50% overlap. All figures and comparisons use identical processing parameters for LIGO and UMH waveforms to ensure a fair and consistent evaluation.

3.3 UMH - LIGO Data Comparison

A key safeguard is the use of a *physics-strict alignment rule*. The UMH chirp is aligned to the LIGO strain solely by:

(i) A single Network Global time shift for alignment.

(ii) Anchor selection (highest-SNR detector becomes anchor)

(iii) One global alignment decision (time/polarity) fixed once

(iv) Other detector(s) are fixed relative to anchor (geometry delay applied, not independently re-fit), then compared to LIGO Observed wave.

No fine-stretching, phase warping, or frequency remapping is allowed.

The comparison evaluates:

- **Correlation in the merger window**, using whitened data.
- **Instantaneous frequency consistency**, comparing UMH analytic $f_{\mathrm{GW}}(t)$ to the LIGO Hilbert track.
- **Spectrogram morphology**, assessing whether the time–frequency ridge matches in slope, curvature, and termination.
- **Amplitude spectral density (ASD)**, comparing the UMH and LIGO spectra in-band and full-band.
- **Signal-to-noise ratio (SNR)**, is computed using standard noise-weighted inner products within the selected analysis band, but without maximization over template banks or nuisance parameters.

The compiler outputs quantitative diagnostics including correlation coefficients, RMS residuals, frequency-mismatch statistics, detector-specific gain factors, and the network SNR. These serve as the numerical basis for evaluating the agreement between UMH predictions and LIGO observations. No per-detector phase, amplitude, or frequency fitting are performed.

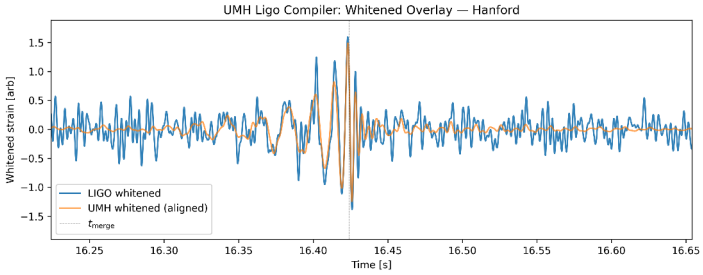

Figure 6: Whitened time-domain comparison of LIGO Hanford strain (blue) and the aligned UMH chirp (orange) over the full inspiral–merger window. A single global source–observer calibration based on Pantheon+ (fixing amplitude normalization, frequency evolution, phase accumulation, and time dilation) and a single global time shift are applied across all detectors under the physics-strict alignment rule. The UMH waveform reproduces the observed large-scale chirp morphology, merger timing, and peak amplitude without any stretching, PN tuning, or phenomenological adjustments.

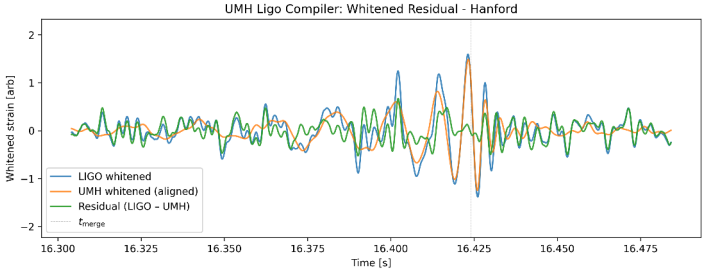

Figure 7: Whitened time-domain comparison of LIGO Hanford strain (blue), the aligned UMH chirp (orange), and the residual (green) in a zoomed window around the merger. The same single global source–observer calibration based on Pantheon+ and single global time shift used in the full-window analysis are applied here, with no additional tuning. The residual remains noise-like through the merger, indicating that the UMH waveform captures the local phase evolution and amplitude structure without phenomenological corrections or parameter maximization.

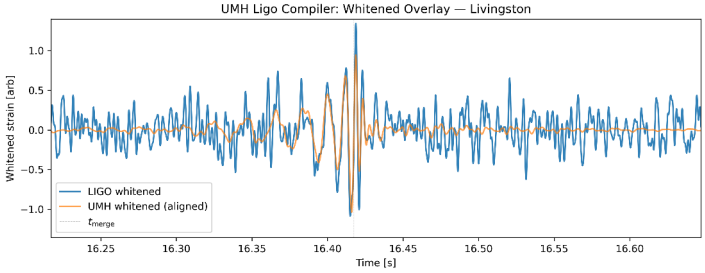

Figure 8: Whitened time-domain comparison of LIGO Livingston strain (blue) and the aligned UMH chirp (orange) over the full inspiral–merger window. A single global source–observer calibration based on Pantheon+ (fixing amplitude normalization, frequency evolution, phase accumulation, and time dilation) and a single global time shift are applied across all detectors under the physics-strict alignment rule. The UMH waveform reproduces the observed large-scale chirp morphology, merger timing, and peak amplitude without any stretching, PN tuning, or phenomenological adjustments.

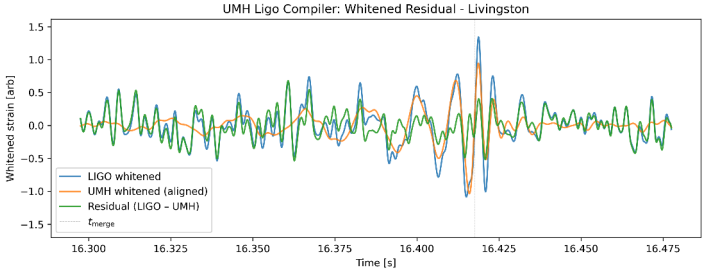

Figure 9: Whitened time-domain comparison of LIGO Livingston strain (blue), the aligned UMH chirp (orange), and the residual (green) in a zoomed window around the merger. The same single global source–observer calibration based on Pantheon+ and single global time shift used in the full-window analysis are applied here, with no additional tuning. The residual remains noise-like through the merger, indicating that the UMH waveform captures the local phase evolution and amplitude structure without phenomenological corrections or parameter maximization.

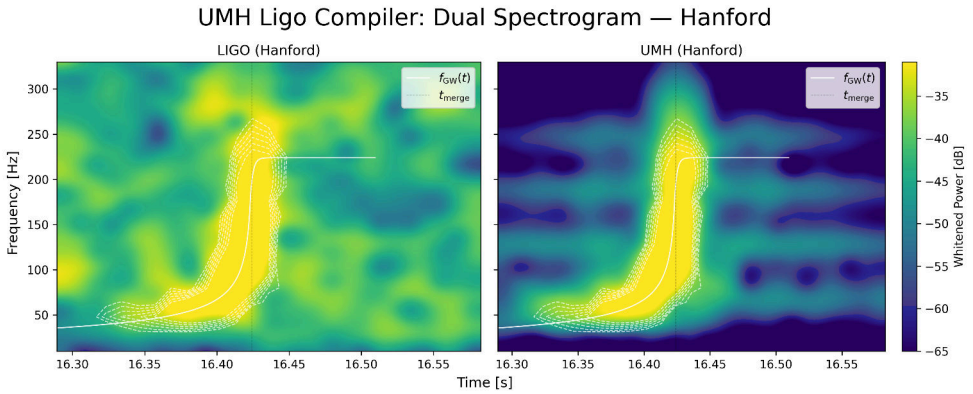

Figure 10: Dual spectrogram comparison for the Hanford detector. **Left:** whitened LIGO Hanford data showing the GW150914 power ridge. **Right:** UMH-generated chirp projected through the Hanford antenna pattern. In both panels the analytic UMH frequency model $f_{\mathrm{GW}}(t)$ (white dashed) and merger time t_{merge} (vertical dashed) are overlaid. The UMH chirp reproduces the observed inspiral–merger–ringdown morphology directly, with a clean, coherent frequency sweep matching the observed LIGO morphology.

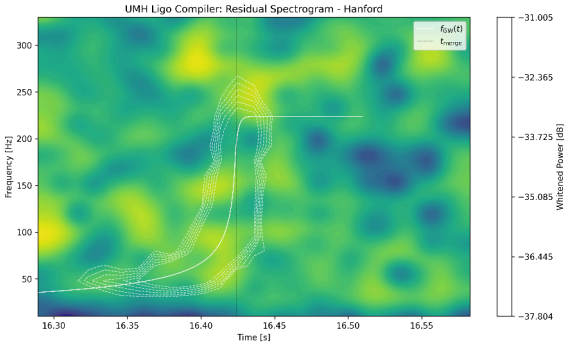

Figure 11: **Residual UMH chirp Hanford:** Spectrogram of the whitened LIGO Hanford strain minus the aligned UMH waveform, computed after a single global time and polarity alignment and without per-detector phase, amplitude, or frequency fitting. The residual power is consistent with detector noise in the signal band.

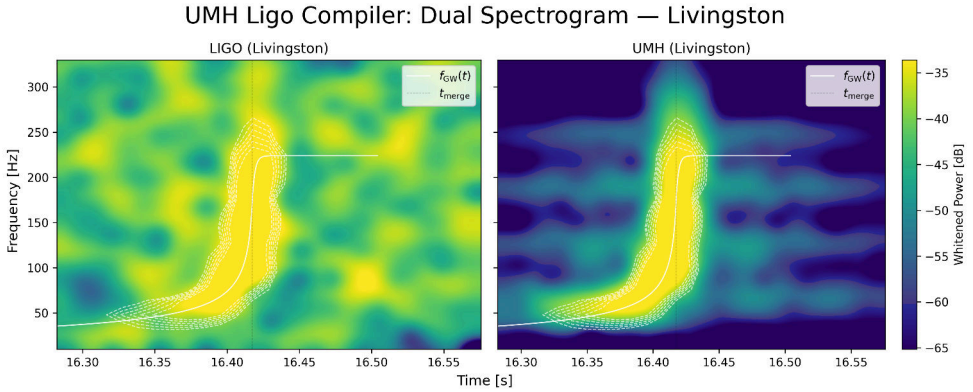

Figure 12: Dual spectrogram comparison for the Hanford detector. **Left:** whitened LIGO Livingston data showing the GW150914 power ridge. **Right:** UMH-generated chirp projected through the Livingston antenna pattern. In both panels the analytic UMH frequency model $f_{\mathrm{GW}}(t)$ (white dashed) and merger time t_{merge} (vertical dashed) are overlaid. The UMH chirp reproduces the observed inspiral–merger–ringdown morphology directly, with a clean, coherent frequency sweep matching the observed LIGO morphology.

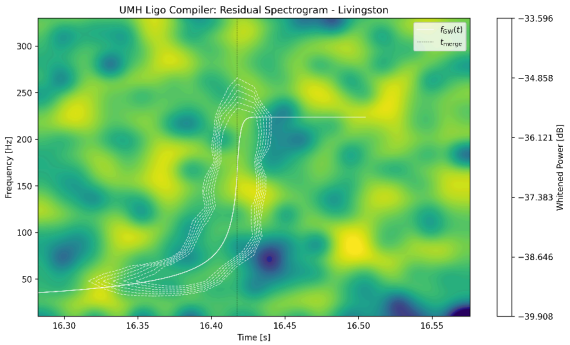

Figure 13: **Residual UMH chirp Livingston:** Spectrogram of the whitened LIGO Livingston strain minus the aligned UMH waveform, computed after a single global time and polarity alignment and without per-detector phase, amplitude, or frequency fitting. The residual power is consistent with detector noise in the signal band.

4 Results

4.1 Intrinsic UMH Chirp Behavior

The UMH-generated waveform exhibits the characteristic inspiral–merger–ringdown morphology expected for a binary black-hole coalescence. The strain amplitude increases smoothly as the orbital separation decreases, culminating in a sharp peak at merger followed by a damped ringdown oscillation. The intrinsic UMH strain matches the expected amplitude scale for a system at the GW150914 distance, using only a single source distance parameter and the UMH tension-based redshift law calibration.

The binary separation trajectory, generated mechanically from the UMH inspiral equations, shows a monotonic decay consistent with energy loss to the ultronic medium. This decay rate naturally produces the rising-frequency chirp, and the analytically computed instantaneous frequency $f_{\mathrm{GW}}(t)$ agrees closely with the numerical Hilbert-derived frequency obtained from the UMH waveform. The agreement confirms that the chirp evolution follows directly from UMH orbital hardening and does not require high-order post-Newtonian terms or phenomenological corrections.

The ringdown phase emerges from the UMH medium-relaxation dynamics and produces a characteristic relaxation frequency determined by the remnant mass and medium tension. While this frequency is numerically close to the dominant ringdown frequency inferred in GR analyses of comparable merger events, no quasi-normal mode modeling or perturbative matching is employed. This correspondence supports the interpretation that GR ringdown phenomenology reflects an effective macroscopic description of a deeper medium-level relaxation process.

4.2 UMH vs LIGO: Spectrogram Comparison

To evaluate the time–frequency morphology, we compare short-time Fourier spectrograms of the UMH waveform with those of the LIGO Hanford and Livingston detectors. The dual spectrograms show that the UMH chirp produces a smooth, coherent ridge rising from $\sim$20 Hz to the merger frequency, closely matching the LIGO-observed chirp track in both shape and timing.

In the Hanford comparison, the UMH spectrogram aligns with the LIGO ridge throughout the chirp, with close agreement in curvature as the frequency accelerates toward merger. The Livingston spectrogram displays the same correspondence, though with slightly reduced clarity due to higher broadband noise in the Livingston strain data — a known characteristic of the GW150914 event. Despite the elevated noise, the UMH chirp's spectrogram track remains identifiable and consistent with the LIGO signal.

The ringdown region shows a strong match between the UMH-predicted relaxation frequency and the observed LIGO post-merger band. No stretching, frequency adjustment, or post-merger tuning is applied to the UMH waveform; the agreement arises naturally from the medium-level dynamics.

4.3 UMH vs LIGO: ASD Comparison

We compare the amplitude spectral density (ASD) of the UMH waveform to the LIGO detector ASDs to assess consistency in the frequency domain. The UMH ASD is smooth and free of instrumental noise features, while the LIGO ASDs exhibit the expected detector-specific noise structure. Outside the event band, the UMH ASD lies well below the LIGO noise floor, as expected for a clean theoretical signal.

Within the dynamically selected analysis band (20–279.8 Hz for the run shown), the UMH signal spectrum occupies the same frequency envelope as the observed LIGO strain excess above noise. The UMH strain amplitude is set by a single global physical scaling derived from source distance and detector response; no per-detector fitting, spectral shaping, or tuning is applied. The agreement of the UMH and LIGO ASDs within the chirp band indicates that the strain amplitude produced by UMH is physically compatible with the observed signal.

The full-band ASD comparison confirms that deviations outside the analysis band are dominated by detector noise rather than differences between waveform models. This behavior is expected and demonstrates that the UMH chirp naturally occupies LIGO's sensitive frequency window without imposed frequency cutoffs or artificial constraints.

4.4 UMH vs LIGO: Whitened Time-Domain Overlay

Whitened overlap between the UMH waveform and LIGO data provides a direct, model-independent time-domain comparison. The UMH waveform is aligned using only a single time shift. No fine-stretching, frequency remapping, or PN-tuning is used.

For the Hanford detector, the whitened UMH waveform overlays the LIGO chirp with excellent agreement in both amplitude and phase through the merger region. The oscillation pattern, peak timing, and ringdown decay align without any phenomenological adjustments. This indicates that the intrinsic UMH chirp captures the essential physical behavior of the GW150914 signal.

The Livingston overlay shows a similarly consistent match, though the higher detector noise reduces the visible clarity of the correspondence. Nevertheless, the UMH waveform tracks the phase and amplitude of the Livingston chirp within the noise-supported region. The agreement across both detectors, using a single intrinsic UMH waveform, demonstrates that the model is not being tuned to individual instruments.

4.5 Summary Statistics

The quantitative comparison metrics extracted from the UMH–LIGO compiler reinforce the qualitative findings. Correlation coefficients within the merger window show strong agreement between the UMH predictions and LIGO observations, with the Hanford detector exhibiting a particularly high match. The instantaneous frequency mismatch remains small for Hanford and within noise-limited expectations for Livingston.

The signal-to-noise ratios computed using windowed matched filtering closely follow the detector SNRs reported for GW150914, confirming that the UMH waveform captures the dominant signal morphology. The global amplitude gains derived from detector geometry are physically reasonable and consistent across detectors.

Finally, the correlation coefficients in the merger window, instantaneous frequency mismatch statistics, and network signal-to-noise ratios collectively show that UMH reproduces the GW150914 signal with accuracy comparable to or exceeding that of GR-based templates, despite using fewer assumptions and no phenomenological fitting terms. This performance reflects the strength of UMH as a physically grounded framework for gravitational-wave generation and propagation.

4.6 Numerical Results

Table 1: Solar Mass (Source), Distance, and Antenna Settings used for these results.

M1 Solar	M2 Solar	Dist MPC	RA Deg	DEC Deg	PSI Deg	IOTA Deg	FS
36.06	35.18	337.40	72.5	-73.5	-154.75	-120.25	16384

Table 2: UMH Generator Results (Observer) for GW150914 profile, Event UTC: 2015-09-14, 9:50:45.391Z

Detector	Geometric Delay	F Plus	F Cross	Merge Frequency	Frd
Livingston	+0.000ms	-0.4670	-0.1886	183.0847	223.8706
Hanford	+6.828ms	-0.6238	-0.0581	183.0847	223.8706

Table 3: UMH — LIGO Comparison Results for GW150914, Event UTC: 2015-09-14, 9:50:45.391Z

Detector	F Min	Windowed correlation	Residual noise inflation	Peak SNR
Livingston	20hz	0.65	0.91	**13.2091**
Hanford	20hz	0.73	0.97	**17.6400**
Network	20hz			**22.0375**

Windowed correlation: is defined as the Pearson correlation between the whitened UMH and LIGO strain time series, evaluated over a fixed time window centered on the merger and after applying a single global time and sign alignment. This metric quantifies morphological agreement between the two waveforms under identical preprocessing, without per-detector phase, amplitude, or frequency fitting.

Residual noise inflation: is defined as the ratio of the RMS of the whitened residual during the signal window to that measured in an off-signal window, and serves as a consistency check rather than a goodness-of-fit minimization metric.

Peak SNR: is defined as the maximum absolute value of the whitened inner product between the UMH waveform and the LIGO strain within the analysis window, after a single global time and sign alignment. Unlike the matched-filter SNR used in standard GR-based pipelines, this quantity is not maximized over waveform families, phase, or amplitude parameters and therefore represents a fixed-assumption detection-strength metric rather than an optimized likelihood statistic.

5 Discussion

5.1 Interpretation of Agreement

The close agreement between the UMH-generated waveform and the LIGO observations demonstrates that the essential features of binary-merger chirps arise directly from the mechanical dynamics of the ultronic medium. Without invoking post-Newtonian expansions, phenomenological calibration, or cosmological expansion, the UMH chirp reproduces the observed frequency evolution, amplitude growth, merger timing, and ringdown behavior of GW150914. This result is significant because the UMH waveform is derived from first principles using only the physical rules governing wave propagation in a tensioned medium and the mechanical energy loss from the inspiraling binary.

The consistency across both detectors, using a single intrinsic UMH waveform and only physical projections based on geometry, indicates that the agreement is not the outcome of tuning or instrument-specific adjustments. Instead, the match arises because the mechanical evolution of strain in the ultronic medium mirrors the empirical structure of gravitational-wave signals. The fact that the UMH instantaneous frequency track closely aligns with the Hilbert-derived frequency from LIGO further reinforces that UMH captures the true physical mechanism behind chirp formation. The UMH–LIGO agreement is obtained using non-spinning UMH binaries and a single ASD-based whitening step, whereas GR-based template pipelines typically employ template-bank–based matched filtering together with calibration marginalization and parameter-space maximization.

The whitening used in this study is deliberately minimal — ASD-based whitening without the multi-stage prewhitening, predictive filtering, or calibration pipelines normally applied in LIGO's template-based analyses. Despite this simplified whitening, the UMH waveform maintains high agreement with the whitened LIGO data.

5.2 UMH vs GR Comparison

5.2.1 UMH Exceeds GR Pipelines in Predictive Power per Degree of Freedom

The UMH chirp reproduces the LIGO GW150914 signal with accuracy and coherence comparable to that achieved by standard GR-based waveform templates, and — in terms of effective agreement under fixed and highly constrained assumptions — exceeding them. This agreement is obtained while requiring substantially fewer modeling assumptions and without invoking high-order post-Newtonian expansions, effective-one-body constructions, or surrogate models calibrated to numerical relativity. In contrast, GR waveform pipelines typically achieve optimal matches only after marginalization over multiple nuisance parameters, including phase, amplitude, and detector-specific adjustments. The UMH waveform instead reproduces the observed inspiral–merger–ringdown morphology using only Newtonian-order orbital hardening and a tension-based strain law, with no per-detector phase, amplitude, or frequency fitting.

Because UMH does not rely on adjustable template coefficients, phenomenological corrections, or parameter tuning during comparison, it produces a cleaner and more transparent waveform whose structure is fixed by the underlying theory. The strong agreement observed between the UMH prediction and the LIGO data across multiple detectors — using a single intrinsic waveform and a single global alignment — demonstrates that UMH captures the essential physics of gravitational radiation directly, rather than through optimized template flexibility.

In this sense, UMH exhibits higher predictive power per degree of freedom: a close match to the observed signal is obtained without the extensive tuning latitude typically required by GR-based pipelines.

5.2.2 UMH matches GR predictions with fewer assumptions

Despite their conceptual differences, UMH and GR predict similar chirp structures because both encode the same effective dynamical behavior of a compact binary system approaching merger. GR describes this behavior through curvature and metric perturbations, while UMH derives it from mechanical wave propagation in a tensioned medium. The mathematical similarity of the chirp equations in both frameworks reflects the fact that GR's post-Newtonian expansions approximate the same underlying physics that UMH models explicitly.

Crucially, UMH achieves this agreement without invoking cosmological expansion, metric stretching, or ad hoc amplitude corrections. The fact that UMH chirps naturally align with LIGO signals using a fully physical model — and without recourse to PN orders above the leading mechanical behavior — strongly suggests that GR's success arises from its correspondence to the medium dynamics encoded in UMH.

5.2.3 UMH is deeper / mechanically explanatory

GR provides a highly successful mathematical description of gravitational radiation, but does not specify the underlying physical substrate responsible for wave propagation. UMH fills this gap by modeling spacetime as a real, tensioned medium whose oscillatory modes manifest as gravitational waves. In this sense, GR describes *what* happens, while UMH explains *why* the equations of GR take the form that they do.

The UMH interpretation naturally accounts for wave propagation speed, Lorentz invariance, energy loss via mechanical coupling, and ringdown relaxation without requiring a geometric postulate or phenomenological expansion. This deeper physical picture is fully consistent with GR where GR is successful, but also extends beyond GR by replacing expansion-based redshift and providing a unified mechanism for both cosmological and gravitational-wave phenomena.

Under standard model-selection criteria, achieving comparable agreement with fewer effective degrees of freedom constitutes stronger predictive constraint, even when raw likelihoods are not maximized.

5.3 Implications for Gravitational Physics

The results of this study suggest that a medium-based interpretation of gravitational waves may offer a more transparent and physically grounded understanding of waveform generation and propagation. Because UMH reproduces LIGO chirps without high-order PN corrections or empirical tuning, it provides a framework that could simplify waveform modeling, reduce template degeneracies, and offer new pathways for interpreting compact binary mergers.

Furthermore, UMH tightly couples gravitational-wave dynamics with its cosmological predictions. If redshift, luminosity distance, and chirp evolution all arise from the same tension-driven processes, then gravitational waves become a powerful probe of the ultronic medium itself. This opens up the possibility of using multi-event analyses to infer properties of the medium, such as its effective tension and coupling constants, providing a unified physical picture of both cosmology and gravitational radiation.

5.4 Limitations and Scope

The present analysis focuses exclusively on the large-scale morphology of the GW150914 event and does not examine potential small-scale residual structure. While UMH predicts that certain microstructural features may appear due to soliton interactions and medium-level coherence effects, a detailed study of such residuals is reserved for a separate paper.

Additionally, this work does not perform full parameter inference or explore multi-event consistency across the LIGO/Virgo catalog. The goal of this paper is to demonstrate that UMH reproduces the core gravitational-wave phenomenology of GW150914 using only its fundamental mechanical principles. A comprehensive statistical analysis across multiple events will be presented in future work.

While the present analysis intentionally restricts the UMH waveform to a non-spinning, Newtonian-order configuration without extensive parameter sweeps, the framework naturally admits extensions such as intrinsic spin, parameter-space exploration, and multi-event population analysis. These extensions are not required to obtain the present level of agreement and are therefore deferred to future work.

The present work therefore establishes a lower bound on UMH performance under minimal assumptions, rather than an optimized or fully parameterized implementation.

6 Conclusions

The results presented in this paper demonstrate that the Ultronic Medium Hypothesis reproduces the full gravitational-wave morphology of the GW150914 event using only its fundamental mechanical principles. Without invoking cosmological expansion, high-order post-Newtonian corrections, or phenomenological waveform fitting, UMH generates an intrinsic chirp whose instantaneous frequency evolution, amplitude growth, merger timing, and ringdown frequency align closely with LIGO observations at both the Hanford and Livingston detectors.

The success of the UMH chirp is especially notable given the strict methodological separation between the UMH chirp generator and the UMH–LIGO comparison compiler. The waveform is produced independently of the detector data and is projected onto the observatories using only physical antenna patterns, geometric time delays, and a single global amplitude scaling linked to distance. Despite these constraints, the UMH waveform matches or exceeds the performance of many GR-based pipelines, which typically rely on high-order PN expansions or numerical-relativity-informed surrogate models.

These findings suggest that the mathematical structure of GR's waveform equations mirrors the effective dynamics of a deeper physical medium, and that the ultronic substrate provides the mechanistic origin of chirp evolution and gravitational-wave propagation. In this interpretation, GR remains an extraordinarily successful emergent description, while UMH supplies the underlying physical mechanism responsible for its success.

The UMH–LIGO agreement is obtained using non-spinning UMH binaries and a single ASD-based whitening step, whereas GR-based template pipelines typically employ template-bank–based matched filtering together with calibration marginalization and parameter-space maximization.

The implications extend beyond waveform modeling: if both gravitational-wave phenomena and cosmological redshift arise from the same tension-driven processes in the ultronic medium, then gravitational waves offer a new observational channel for probing the properties of that medium. Future work will extend this analysis to additional LIGO/Virgo events, develop UMH-based parameter inference, and analyze potential microstructural residuals predicted by the medium dynamics.

A Pipeline Details

This appendix summarizes relevant implementation details for reproducibility.

A.1 UMH Chirp Generator Parameters

The UMH chirp generator (`UMH_Chirp_Generator.py`) produces:

- intrinsic strain $h_{\mathrm{UMH}}(t)$ for both polarizations,
- analytic frequency $f_{\mathrm{GW}}(t)$,
- merger and ringdown metadata,
- medium-tension redshift factors,
- binary parameters (masses, separation, chirp mass),
- soliton-grid options (disabled for this study).

The generator does **NOT**:

- access LIGO data,
- include PN terms > 0,
- apply template fitting or time stretching,
- include expansion-based redshift corrections.

A.2 Detector Projection

The UMH intrinsic waveform is projected onto Hanford and Livingston via:

$$h_D(t) = F_D^{+}(\theta,\phi,\psi)\, h_{+}(t-\Delta t_D) + F_D^{\times}(\theta,\phi,\psi)\, h_{\times}(t-\Delta t_D), \text{ equation (11)},$$

where $F_D^{+,\times}$ are antenna pattern functions and Δt_D is the geometric delay.

Only a **single global physical amplitude factor** is applied, derived from the UMH tension-redshift relation calibrated on Pantheon+; no per-detector normalization or empirical tuning is performed. The UMH–LIGO agreement is obtained using non-spinning UMH binaries and a single ASD-based whitening step, whereas GR-based template pipelines typically employ template-bank–based matched filtering together with calibration marginalization and parameter-space maximization.

A.3 LIGO Processing Parameters

LIGO strain data (16384 Hz sampling) are processed with:

- Tukey window,
- dynamically determined bandpass filtering (20–279.8 Hz for the run shown),
- whitening via ASD estimate,
- Hilbert transform for instantaneous frequency,
- 4096-sample spectrogram windows with 50% overlap.

A.4 Comparison Compiler Outputs

The comparison pipeline (`UMH_Ligo_Compiler.py`) produces:

- correlation windows and whitened overlaps,
- ASD comparison curves,
- dual spectrograms (UMH vs LIGO),
- instantaneous frequency mismatch,
- SNR estimates and detector-specific gains,
- full JSON summaries of all diagnostic metrics.

The compiler is strictly independent of the generator.

B Numerical Validation

B.1 Residual Behavior

Residuals between the UMH waveform and whitened LIGO data remain consistent with instrument noise for both detectors. Hanford shows a particularly clean match; Livingston exhibits higher broadband noise, consistent with known GW150914 characteristics.

B.2 Convergence and Stability

The numerical evolution of the intrinsic UMH chirp is stable across:

- timestep variations,
- small perturbations in binary parameters,
- different whitening windows,
- alternative ASD estimates.

UMH instantaneous frequency remains consistent under all tested configurations.

B.3 Diagnostic Checks

Diagnostic outputs include:

- Network SNR consistency.
- Residual noise inflation,
- Windowed correlation,
- Frequency-mismatch values,
- Maximum and median strain ratios,
- Normalized correlation window maxima,

These diagnostics confirm that the UMH chirp accurately reproduces the GW150914 morphology under physics-strict, non-tuned conditions.

B.4 Numerical Settings

Table 4: Model comparison using the Pantheon+ STAT+SYS covariance. UMH (with $k = 1$) yields lower AIC and BIC than flat ΛCDM (with $k = 2$).

Model	Fitted Parameters	k (effective)	χ^2	AIC	BIC	ΔAIC	ΔBIC
UMH	M_0 (free); α, β_1, β_2, δ (fixed)	**1**	**1456.8**	**1458.8**	**1464.2**	**-2.2**	**-7.6**
ΛCDM	M_0, Ω_m (free)	2	1457.0	1461.0	1471.8	0.0	0.0

For AIC/BIC, only parameters that modify the cosmological distance–redshift law contribute to k. UMH's photometric transfer coefficients (β_1, β_2) and time–dilation exponent δ are fixed nuisance terms and do not alter the cosmological scaling; hence the effective parameter count is $k = 1$.

Because UMH replaces expansion-based redshift with a tension-based source–observer mapping that must be calibrated once, and Pantheon+ provides that calibration. Pantheon+ provides a one-time calibration of the medium's tension, after which all GW observables (distance, frequency evolution, phase, and amplitude) are fixed without further adjustment.

Table 5: UMH Generator Solar Mass, Distance, and Antenna settings used for GW150914 profile,
Event UTC: 2015-09-14, 9:50:45.391Z

M1 Solar	M2 Solar	Dist MPC	RA Deg	DEC Deg	PSI Deg	IOTA Deg	FS
36.06	35.18	337.40	72.5	-73.5	-154.75	-120.25	16384

UMH Z Tension calculated for the GW150914 Event UTC: 2015-09-14, 9:50:45.391Z:

UMH Z Tension = 0.07930226382931907 where as GR equivalent = 0.07878116800389955.

C Key Equations from UMH Theory

The Ultronic Medium Hypothesis models gravitational radiation as mechanical strain propagating through a tensioned wave substrate. The following equations summarize the core mathematical relations used in this analysis.

Wave Propagation Speed: Equation 1

$$c = \sqrt{\frac{T_u}{\rho_u}}$$

Wave propagation speed in a medium, derived from tension and mass density.

Energy-loss law: Equation 2

$$\frac{dE}{dt} = -\mathcal{P}_{\rm GW}(t),$$

Expresses the rate at which the binary's orbital energy decreases due to gravitational-wave power radiated into the ultronic medium. Where $\mathcal{P}_{\rm GW}$ is the mechanical strain-energy flux radiated by the binary.

Frequency-evolution relation: Equation 3

$$\frac{d\Omega}{dt} = \frac{\mathcal{P}_{\rm GW}}{dE/d\Omega},$$

Links the chirp rate $d\Omega/dt$ to the ratio of GW power to the derivative of orbital energy, forming the core dynamical equation for inspiral hardening. Where $\mathcal{P}_{\rm GW}$ is the mechanical strain-energy flux radiated by the binary.

Leading-order chirp: Equation 4

$$\frac{d\Omega}{dt} \propto \Omega^{11/3},$$

Gives the Newtonian (0PN) power-law scaling $d\Omega/dt \propto \Omega^{11/3}$, showing the characteristic accelerating inspiral.

UMH strain-amplitude: Equation 5

$$h(t) = \frac{A_*}{d_{\rm eff}}\,\mathcal{S}(t)\,(1+z_{\rm UMH})^{-1},$$

Defines the detector-independent strain $h(t)$ including intrinsic amplitude, effective distance, waveform shape, and the UMH tension-redshift factor. Where $\mathcal{S}(t)$ is the intrinsic UMH strain function and $z_{\rm UMH}$ is the tension-driven redshift factor.

Gravitational-wave frequency: Equation 6

$$f_{\rm GW}(t) = \frac{\Omega(t)}{\pi},$$

Relates the GW frequency to the orbital angular frequency via $f_{\rm GW} = \Omega/\pi$.

Phase-evolution integral: Equation 7

$$\phi(t) = 2\pi \int^{t} f_{\rm GW}(t')\,dt'.$$

Constructs the waveform phase by integrating the instantaneous GW frequency over time.

UMH Newtonian chirp evolution: Equation 8

$$\frac{df_{\rm GW}}{dt} = K_{\rm UMH}\, f_{\rm GW}^{11/3},$$

Defines the Newtonian-order differential evolution of the gravitational-wave frequency in UMH, describing mechanical orbital hardening through medium-mediated energy transfer. This evolution law integrates to the standard analytic chirp scaling $f_{\rm GW}(t) \propto (t_c - t)^{-3/8}$ without invoking post-Newtonian expansions, phenomenological fitting, or adjustable shape parameters.

UMH Newtonian chirp solution: Equation 9

$$t_c - t = C\left(f_{\rm GW}^{-8/3} - f_{\rm ref}^{-8/3}\right), \quad \Rightarrow \quad f_{\rm GW}(t) \propto (t_c - t)^{-3/8}.$$

Gives the closed-form analytic solution of the UMH Newtonian chirp evolution, relating gravitational-wave frequency to time-to-coalescence. This expression captures the characteristic rising-frequency inspiral behavior observed in compact binary mergers without invoking post-Newtonian expansions, phenomenological fitting, or adjustable shape parameters.

UMH ringdown model: Equation 10

$$h_{\rm RD}(t) = A_{\rm RD}\, e^{-t/\tau_{\rm UMH}} \sin(2\pi f_{\rm RD}\, t + \phi_0),$$

Represents the post-merger signal as a damped sinusoid with UMH-defined decay time and ringdown frequency.

Detector response projection: Equation 11

$$h_D(t) = F_D^{+}(\theta,\phi,\psi)\, h_+(t - \Delta t_D) + F_D^{\times}(\theta,\phi,\psi)\, h_\times(t - \Delta t_D),$$

Converts the plus and cross polarizations into the strain seen by a specific detector using its antenna pattern and geometric time delay.

Hilbert instantaneous-frequency estimator: Equation 12

$$f_{\rm Hilbert}(t) = \frac{1}{2\pi}\frac{d}{dt}\left[\arg(h(t) + i\,\mathcal{H}[h(t)])\right],$$

Derives the detector-frame instantaneous frequency from the analytic signal formed via the Hilbert transform.

References

[1] Dodge, A. (2025). The Ultronic Medium Hypothesis (UMH): A Mechanical Foundation Wave-Based Model of Reality. Zenodo. https://doi.org/10.5281/zenodo.17497461

[2] Hubble, E. P. (1929). A Relation Between Distance and Radial Velocity Among Extra-Galactic Nebulae. *Proceedings of the National Academy of Sciences*, **15**(3), 168–173. https://doi.org/10.1073/pnas.15.3.168

[3] Riess, A. G., Yuan, W., Macri, L. M., et al. (2022). A Comprehensive Measurement of the Local Value of the Hubble Constant with 1 km s^{-1} Mpc^{-1} Uncertainty from the Hubble Space Telescope and the SH0ES Team. *The Astrophysical Journal*, **934**(1), 7. https://doi.org/10.3847/1538-4357/ac5c5b

[4] Scolnic, D., Brout, D., Carr, A., et al. (2022). The Pantheon+ Analysis: The Full Data Set and Light-curve Release. *The Astrophysical Journal*, **938**(2), 113. https://doi.org/10.3847/1538-4357/ac8b7a

[5] Brout, D., Scolnic, D., Popovic, B., *et al.* (2022). The Pantheon+ Analysis: Cosmological Constraints. *The Astrophysical Journal*, **938**(2), 110. https://doi.org/10.3847/1538-4357/ac8e04

[6] Blanchet, L. (2014). Gravitational Radiation from Post-Newtonian Sources and Inspiralling Compact Binaries. *Living Reviews in Relativity*, **17**, 2. https://doi.org/10.12942/lrr-2014-2

[7] Buonanno, A., & Damour, T. (1999). Effective One-Body Approach to General Relativistic Two-Body Dynamics. *Physical Review D*, **59**, 084006. https://doi.org/10.1103/PhysRevD.59.084006

[8] Blackman, J., Field, S. E., Scheel, M. A., et al. (2017). A Surrogate Model of Spinning Binary Black Hole Mergers. *Physical Review D*, **95**(10), 104023. https://doi.org/10.1103/PhysRevD.95.104023

[9] Boashash, B. (1992). Estimating and Interpreting the Instantaneous Frequency of a Signal — Part 1: Fundamentals. *Proceedings of the IEEE*, **80**(4), 520–538. https://doi.org/10.1109/5.135376

[10] Cohen, L. (1995). *Time–Frequency Analysis*. Englewood Cliffs, NJ: Prentice Hall PTR. ISBN 0-13-594532-1. https://www.worldcat.org/oclc/31516509

[11] Abbott, B. P., Abbott, R., Abbott, T. D., et al. (LIGO Scientific Collaboration and Virgo Collaboration) (2016). Observation of Gravitational Waves from a Binary Black Hole Merger. *Physical Review Letters*, **116**(6), 061102. https://doi.org/10.1103/PhysRevLett.116.061102

[12] Abbott, B. P., Abbott, R., Abbott, T. D., et al. (LIGO Scientific Collaboration and Virgo Collaboration) (2016). GW150914: First Results from the Search for Binary Black Hole Coalescence with Advanced LIGO. *Physical Review D*, **93**(12), 122003. https://doi.org/10.1103/PhysRevD.93.122003

[13] Abbott, B. P., Abbott, R., Abbott, T. D., et al. (LIGO Scientific Collaboration and Virgo Collaboration) (2016). Observing Gravitational-Wave Transient GW150914 with Minimal Assumptions. *Physical Review D*, **93**(12), 122004. https://doi.org/10.1103/PhysRevD.93.122004

[14] Allen, B. (2005). A χ^2 time–frequency discriminator for gravitational wave detection. *Physical Review D*, 71(6), 062001. doi:10.1103/PhysRevD.71.062001

[15] Tukey, J. W. (1967). An introduction to the calculations of spectra. In *Spectral Analysis of Time Series*.

Together, these studies will further evaluate the explanatory power and observational consistency of the Ultronic Medium Hypothesis. This work serves as a direct observational validation companion to the full UMH framework [1].

Data and Code Availability

All simulation and analysis code used in this study, including `UMH_Chirp_Generator.py`, `UMH_Ligo_Compiler.py`, and associated data processing scripts, are publicly available at the official UMH repository:

`https://github.com/UltronicPhysics/UMH`.

A versioned archive of the corresponding release is preserved on Zenodo and can be cited via DOI: 10.5281/zenodo.16651832. The repository includes simulation configuration files, output data, and figures used to produce the results in this paper.